PREDICTION OF PLASMA SHEET ELECTRONS EFFECTS ON X-RAY MIRROR MISSIONS

A. Hilgers[1] P. Gondoin[2], P. Nieminen[1], and H. Evans[1]

[1] *Space Environments and Effects Analysis Section,*
Technical and Operational Support Directorate
[2] *Astrophysics Division, Space Science Department*
European Space Research and Technology Centre, European Space Agency,
Noordwijk, The Netherlands, NL-2200 AG.

ABSTRACT

Magnetospheric and interplanetary electrons can affect imaging through X-ray grazing incidence telescopes. Electrons can enter the mirror shells and generate a background signal in the focal plane detectors or interact with the mirror material hereby producing X-ray fluorescence or bremsstrahlung emission. An analytical model is presented which evaluates these effects using an electron flux model in the range 0.1 keV to several MeV derived from ISEE-2 measurements. This provides an upper bound of the expected level of particle induced background in an X-ray mirror mission. This study shows that monitoring of the energetic plasma environment in parallel with X-ray imaging or spectroscopy instrumentation is necessary to interpret low flux X-ray measurements data.

Key words: Plasmasheet; X-ray mirror; radiation effect.

1. INTRODUCTION

X-ray telescopes using grazing incidence mirrors are sensitive to magnetospheric and interplanetary electrons. The design of such grazing incidence telescopes is shown in Figure 1. It consists of Wolter I mirror shells nested in a coaxial and cofocal configuration. Wolter I telescopes are used in all soft X-ray space missions. Interplanetary and magnetospheric electrons can propagate between their mirror shells. They can either reach the focal plane detector or generate X-rays by interaction with the mirror materials. Both effects can contribute to an artificial X-ray background on e.g CCD detectors specially if the electron energy is in the energy bandpass of the focal plane instruments. The electron propagation through grazing incidence mirror has been investigated in previous studies [Danner, 1993] sometimes using Monte-Carlo simulations [Sumner and Lieu, 1990]. Interaction of electrons with mirror materials seems not to have been discussed in the literature. In the present study, the magnitude of both effect is estimated assuming that the reflections of the electrons is specular. Simple analytical expressions are established which provide upper limits of the level of expected particle induced background (PIB hereafter). They use a model of the input electron flux derived from ISEE-2 measurements [*Loidl et al.*, 1996]. The analytical model, the description of the particle environment and the derivation of the PIB are discussed in the following sections.

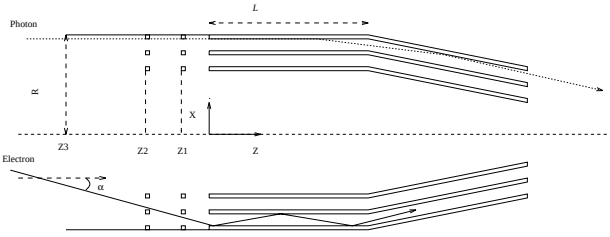

Figure 1. Wolter I design of an X-ray telescope. X-ray baffle sieves have been placed at $Z = Z_1$ and $Z = Z_2$ to reduce X-ray stray-light.

2. ANALYTICAL MODEL

The model assumes that all reflections are specular with a coefficient of reflection η which depends on the angle of incidence, θ, and on the reflective coating material as follows [*Shimizu*, 1974].

$$\eta(\theta) = \exp(\mathrm{Log}(\eta_0)\cos(\theta)) \tag{1}$$

Most electrons entering the telescope first impact the mirror close to the entrance aperture. Hence, the probability for an electron to reach the depth z is given by

$$B(\alpha, w, z, i) = \exp\left(-\mu(z)\frac{\sin^2(\alpha)}{\cos(\alpha)}\right) \text{ if } z \leq L \tag{2}$$

and

$$B(\alpha, w, z, i) = \exp\left(-\mu(L)\frac{\sin^2(\alpha)}{\cos(\alpha)} - \mu(x-L)\frac{\sin^2(\alpha \pm \gamma)}{\cos(\alpha \pm \gamma)}\right) \text{ if } z > L$$

with

$$\mu(s) = -s\mathrm{Log}(\eta_0)\cos\phi/(2\delta) \tag{3}$$

where $\mathrm{Log}(\eta_0)$ is the average logarithmic value of the reflection coefficient, L is the mirror length, γ is the angle between the parabola and the hyperbola section of the Wolter I shells, α is the angle between the particle velocity vector and the mirror optical axis and ϕ is the angle between the projection of the velocity vector in a plane perpendicular to the mirror axis and the perpendicular to the mirror surface at

the incidence point. The electron flux parallel to the mirror axis at depth z can be written as follows.

$$F_1 = \iiint g(w) \sin\alpha \cos\alpha A(\alpha, \phi, i) B(\alpha, w, z, i) d\phi d\alpha dw \quad (4)$$

where $g(w)$ is the differential flux of the particles with energy w (assuming an isotropic velocity distribution), $A(\alpha, \phi, i)$ is the density function of solid angle within which particles from the free space may access the mirror entrance, and $B(\alpha, w, z, i)$ is the density of probability that a particle entering the mirror system with a polar angle α propagates to the location z.

To compare with previous results the effective solid angle of the mirror

$$E = 8 \iint \sin\alpha \cos\alpha B(\alpha, w, z, i) d\phi d\alpha \quad (5)$$

is derived. The present analytical model gives a value of E one to two order of magnitude larger than the Monte-Carlo simulation of *Sumner and Lieu* [1990]. The effect of the non-specular reflection especially on the rough backside of the mirrors could explain this discrepancy. However, the present analytical model performs better than the grazing incidence model of *Danner* [1993] which strongly underestimates the total electron flux propagating between the mirrors.

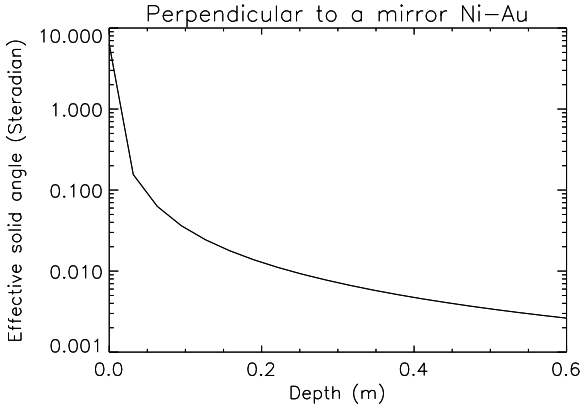

Figure 2. Effective solid angle for the flux perpendicular to a mirror shell derived from the analytical model.

The electron flux perpendicular to the mirror axis at depth z can be written as follows.

$$F_2 = \iiint g(w) \sin\alpha \cos\phi A(\alpha, \phi, i) B(\alpha, w, z, i) d\phi d\alpha dw \quad (6)$$

A useful insight to the process is given by the parameter

$$E_p = 8 \iint \sin\alpha \cos\phi B(\alpha, w, z, i) d\phi d\alpha \quad (7)$$

E_p is shown in Figure 2 as a function of z for a gold coated mirror on a nickel substrate. E_p is a strongly decreasing function of z with its value reduced by one order of magnitude over the first centimeter. Therefore, the PIB which is proportional to the integral of E_p over the mirror length will be mainly due to photons generated over the first few centimeters of the mirrors.

3. DERIVATION OF THE PIB

In space X-ray telescope, magnetic deflectors are often used in the exit telescope aperture to divert soft energy electrons reflected by the mirrors away from the focal plane detectors. The main source of PIB then become the X-ray fluorescence or bremsstrahlung emission induced by the interaction of magnetospheric electrons with the mirror material. The general expression of the PIB due to the flux perpendicular to the shell is

$$\frac{\partial N}{\partial u} = \Sigma_i 2\pi r_i \iiiint g(w) \sin\alpha \cos\phi A(\alpha, \phi, i) B(\alpha, w, z, i) C(\alpha, \phi, w, u, \epsilon) \pi D(z, i, u) d\phi d\alpha dz dw \quad (8)$$

where i is the mirror number. r_i is the radius of mirror i. $C(\alpha, w, u, \epsilon)$ is the density of probability per steradian and eV that a particle with a polar angle α and energy w emits a photon with energy u and polar angle ϵ. $D(z, i, u)$ is the density of probability that a photon emitted at location z inside mirror number i and with energy u reaches the detector.

The PIB has been calculated by *Hilgers et al.* [1998] in the case of the XMM mission [*Gondoin et al.* 1994]. Analytical models of the function A and of the function D have been developed taking into account the presence of X-ray baffles. A simple expression of the function C derived from simulations using the particle transport GEANT code [*GEANT*, 1993] could only be derived for the bremsstrahlung emission. Therefore, only the continuum component of the PIB could be modelled without contribution from the line fluorescence emission. These are however affecting much narrower spectral ranges close to the gold L and M edges.

4. PARTICLE ENVIRONMENT

The electron flux as measured with the ISEE-2 spacecraft is highly variable (see Figure 3). High flux values are observed for particles with energy of 10 keV and above.

High flux values are expected to occur in the narrow domain of the plasmasheet. Close to Earth, the plasmasheet has a thickness of 10 to 12 R_E. Further out its thickness decreases to about 6 to 8 R_E around $X_{GSE} = -20$ R_E [*Baumjohann* 1993]. The position of the plasmasheet undergoes diurnal and annual variations due to the change of the Earth magnetic dipole inclination with respect to the solar wind speed. Sporadic variations are associated with storms and substorms during which the plasmasheet is thinning and expanding. In this study, a statistical model of the electron flux from flux measurements as a function of GSE coordinates is derived without discriminating sporadic from diurnal or annual variations. The model therefore overestimates the spread of the plasmasheet. A better model of the plasmasheet would require more data to improve statistics. Modeling of

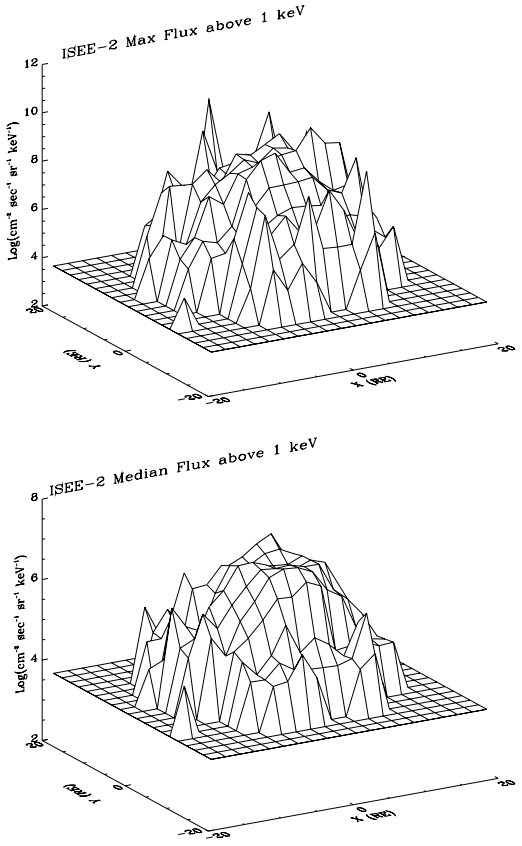

Figure 3. Maximum (top panel) and median (bottom panel) values of the electron flux derived from ISEE-2 as a function of the spacecraft position

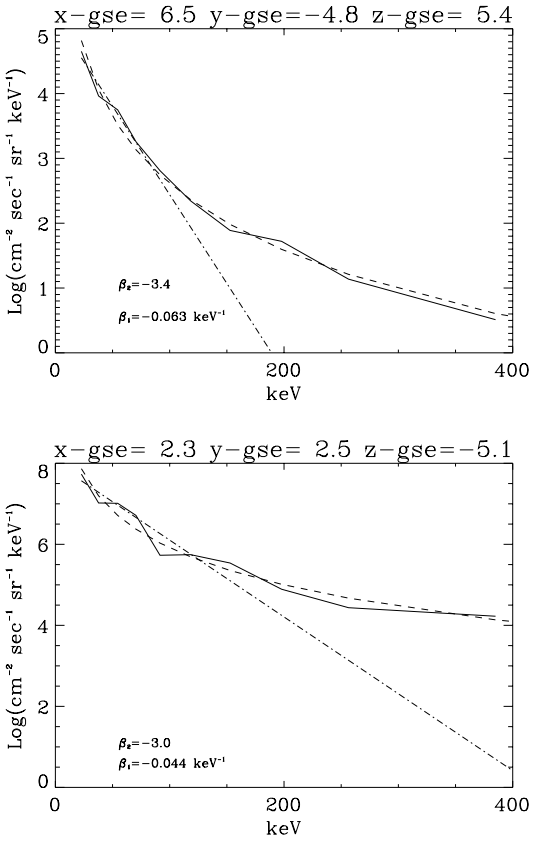

Figure 4. Electron spectra measured in the magnetosphere with ISEE-2. The dashed line represents a power law fit whereas the dotted-dashed line represents a fit of the lower energy range by an exponential.

the plasmasheet is actually a full research topic, a summary of which is given by *Baumjohann* [1993].

Examples of 20-400 keV spectra measured by ISEE-2 in the magnetosphere are shown in Figures 4. In order to evaluate the particle induced X-ray background in the range 0.1 to 15 keV, the measured electron flux must be extrapolated down to 0.1 keV and above 400 keV. In the high energy range above 400 keV, the electron flux was extrapolated using a power law distribution. In the low energy range, we extrapolate the measurements using an exponential distribution since most of the particles are thermalized by wave particle interactions. Finally, the ISEE-2 spectra were fitted by the following analytical expressions.

$$g(w) = g_0 \exp(-\beta_1 w) \text{ for } w < 30 \text{ keV} \qquad (9)$$

and

$$g(w) = g_1 w^{-\beta_2} \text{ for } w > 30 \text{ keV}$$

The extrapolated flux is of the same order of magnitude as the measured flux. Statistical information of the flux integrated above various energy threshold is given Table 1. The values correspond to the maximum, minimum and median values observed above 40,000 km altitude with ISEE-2. The median flux is defined as the value above which the probability of occurrence equals to 50%.

Table 1: ISEE-2 e^- flux above 40,000 km altitude.

Energy	Flux in $cm^{-2}sec^{-1}sr^{-1}$		
threshold (keV)	Maximum	Median	Minimum
0.1	$1.4\,10^{10}$	$1.3\,10^{5}$	$4.9\,10^{4}$
1	$1.3\,10^{10}$	$1.2\,10^{5}$	$4.9\,10^{4}$
8	$7.2\,10^{9}$	$8.9\,10^{4}$	$4.8\,10^{4}$
10	$6.0\,10^{9}$	$8.1\,10^{4}$	$4.7\,10^{4}$

Two dominant electron populations exist outside the magnetosphere. These are the solar wind electrons with temperature of the order of 1 eV and the relativistic Jovian electrons. The energy range of solar wind electrons is not relevant to this study and the background relativistic electrons at 1 AU can be fitted with a power law distribution as follows [Eraker 1982].

$$g(w) = g_2 w^{-\beta_3} \qquad (10)$$

with $g_2 = 2\ cm^{-2}sec^{-1}sr^{-1}keV^{-1}$ and $\beta_3 = 1.7$. This corresponds to an integrated flux above 1 keV equals to 2.9 $cm^{-2}sec^{-1}sr^{-1}$. The same law was used down to 0.1 keV. This assumption likely overestimates the flux in the low energy range. During solar magnetic field conjunction between Earth and Jupiter magnetospheres (every 30 months), flux enhancements of up to one order of magnitude are observed. In addition, sporadic solar particle events lead to relativistic electron flux enhancements by 2 to 3 orders of magnitude with a higher spectral coefficient [Chenette, 1980].

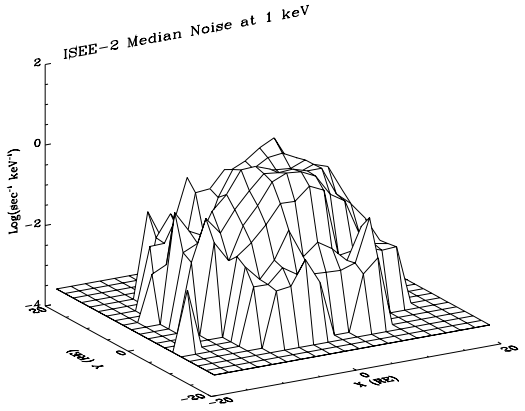

Figure 5. Median value of the bremsstrahlung induced background at 1 keV as deduced from ISEE-2.

The median value of the PIB in the XMM telescope focal plane at 1 keV is shown as a function of the location in a GSE coordinate system in Figure 5 as derived from equation (8). The background is everywhere lower than the X-ray background which is of the order of a few cts $\sec^{-1}\mathrm{keV}^{-1}$ within the XMM telescope field of view.

Table 2: Prediction of PIB in XMM telescope FOV.

Photon Energy (keV)	$\partial N/\partial u(\sec^{-1}\mathrm{keV}^{-1})$ magnetospheric highest	median	lowest	XRB ($\sec^{-1}\mathrm{keV}^{-1}$)
0.1	$2\ 10^2$	$2\ 10^{-2}$	$5\ 10^{-3}$	≥ 10
0.2	$5\ 10^2$	$5\ 10^{-2}$	10^{-2}	≥ 10
1	10^3	10^{-1}	$4\ 10^{-2}$	2.
8	$2\ 10^2$	$2\ 10^{-2}$	10^{-2}	$4\ 10^{-2}$
10	6.	$8\ 10^{-4}$	$5\ 10^{-4}$	$2\ 10^{-2}$

The median, lowest and highest value of the bremsstrahlung background induced in the XMM telescope focal plane at 1 keV is given in table 2 over the whole domain explored by ISEE at altitudes above 40,000 km. PIB predictions in the interplanetary medium are always below the lowest magnetospheric flux. Table 2 indicates that, most of the time and over the whole energy range of the XMM X-ray focal plane cameras, the electron induced background is significantly lower than the cosmic X-ray background, XRB, reported in the last column of Table 2. However, due to the extremely high variability of the magnetospheric electron flux, it is shown that instantaneous peak values may exceed this cosmic background level although during rare instants.

5. CONCLUSION

The simple models described in this paper calculate the ambient electron flux which can propagate through X-ray telescopes. Although they overestimate the exit flux parallel to the telescope axis compared with more detailed Monte-Carlo simulations, they are computationally less heavy. The combination of the simple particle transport models with electron environment model of the type proposed in this study allow to estimate the bremsstrahlung induced background in the focal plane detectors of X-ray telescopes. In the case of XMM, these models demonstrated that most of the time and over the whole energy range of the X-ray cameras, the electron induced background will be lower than the cosmic X-ray background. However, instantaneous peak fluctuations of the electron flux in the near Earth space environment could induce a bremsstrahlung background which may sporadically exceed the cosmic background level for rare instants. In particular, measurements of very faint X-ray sources could be affected for short periods during crossing of the plasmasheet by the spacecraft. On X-ray space observatories, instrument monitoring the electron environment in the range 100 eV to 10 keV can identify those periods. If necessary, the associated events can be filtered out thus improving the overall quality of the X-ray scientific data.

Future work is planned in collaboration with Rutherford Appleton Laboratory to use an extended data set and to characterize electron fluxes during plasma sheet crossing [SEDAT, 1998]. Instruments monitoring the electron environment such as the radiation monitor on board XMM would prove very useful to verify particle transport and electron environmental models such as the ones presented in this study.

REFERENCES

Baumjohann, W., The near-earth plasma sheet: an amptee/irm perspective, *Sp. Sci. Rev., 64*, 141-163, 1993.

Chenette, D. L., The propagation of Jovian electrons to Earth, *J. Geophys. Res, 85*, A5, 2243, 1980.

Danner, R., Charged particle induced background expected in X-ray detecting CCDs in highly eccentric earth orbits, *Experimental Astronomy, Vol. 4*, pp 105-116, 1993.

Eraker, J. H., Origins of the low-energy relativistic interplanetary electrons, *Astroph. J., 257*, 862-880, 1982.

GEANT, Detector Description and Simulation Tool, CERN Program Library Long Writeup W5013, CERN, Geneva, 1993.

Gondoin, P., D. de Chambure, K. van Katwijk, P. Kletzkine, D. Stramaccioni, B. Aschenbach, O. Citterio, R. Willingale, The XMM telescope, *SPIE Proc.2279*, pp.86-100, 1994.

Hilgers, A., P. Gondoin, P. Nieminen, and H. Evans, X-ray background induced by electron bremsstrahlung emission in XMM telescopes: environmental input data and mathematical model, *ESA-WP-1942*, Noordwijk, the Netherlands, Oct. 1998.

Loidl, G. D., E. Keppler, and R. Friedel, Analysis of ISEE data, *Technical note 1 performed for ESTEC under Contract No 10725/94/NL/JG*, April 1996.

SEDAT, Space Environment and Analysis Tools, http://www.wdc.rl.ac.uk/sedat/ ,Contract No 12854/98/NL/NB, 1998.

Shimizu R., *Secondary electron yield with primary electron beam of kilo-electron volts*, J. Applied Phys., Vol. 45, pp 2107, 1974.

Sumner, T. J. and R. Lieu, *Soft-electron background in X-ray telescopes using Wolter I grazing incidence optics in near-Earth orbits*, Optical Engineering, Vol. 29, No 10, pp 1291-1294, Oct. 1990.